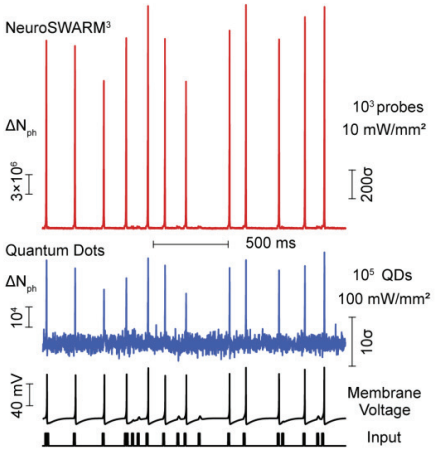

Fig. 4. Simulated electrophysiological recordings with NeuroSWARM^3 and quantum dots (QDs). A phasic spiking Izhikevich model is used for the neural spiking activity at pseudo-random times. The input and resulting membrane voltage are shown (bottom, black). Differential scattering signal detected from 10^3 NeuroSWARM^3 probes (red, top) is shown assuming a light intensity of 10 mW/mm^2 at 1050 nm. Differential fluorescence signal obtained from 10^5 CdSe quantum dots is compared for an illumination intensity of 100 mW/mm^2 (middle, blue). A maximum extracellular field of 3 mV/nm is assumed. Scales indicating the photon count for the differential signal and the standard deviation due to the shot noise are shown on the left and right, respectively.

is the percentage change in the fluorescence lifetime of the decaying excitations. QDs (1.2 nm^2 cross section) are illuminated with 100 mW/mm^2 visible light (650 nm) [20]. Resulting traces show that individual Neuro-SWARM^3 probes (Fig. 4, red) readily outperform QDs (Fig. 4, blue) by providing at least four orders of magnitude enhanced photon-count measurements (left axis), despite the use of 10-fold reduced light intensity (10 mW/mm^2). The fundamental detection limit to any optical measurement technique is the shot noise limit SSNR $\sim (\Delta S/S_0)\sqrt{N_{ph}}$, where $\Delta S/S_0$ is the differential scattering signal and N_{ph} is the photon count. As show in Fig. 4, a remarkably high SSNR measurement capability (SSNR $\sim 10^3$) is achieved due to drastically higher photon-count signals obtained from the Neuro-SWARM^3 (right axis).

V. Conclusion

Neuro-SWARM^3, a system-on-nanoparticle probe, enabling wireless detection of bioelectric signals with single neuron resolution is shown. Neuro-SWARM^3 merges wireless power transfer, electrophysiological signal detection and data broadcasting capabilities in a core-shell nanoparticle structure. It offers high SSNR ($\sim 10^3$) measurements from single neurons within the biologically transparent near-infrared window (NIR II 1000-1700 nm) for non-invasive neural recordings through the skull. Neuro-SWARM^3 technology can open up new horizons for brain-machine interfaces. Integration of NIR Neuro-SWARM^3 with functional spectroscopy could lead to an all-optical methodology, allowing simultaneous detection and distinguishing of the fast neuronal signals (Neuro-SWARM^3) and the slow hemodynamic activity (fNIRS).

References

[1] V. Marx, "Neurobiology: Rethinking the electrode," *Nature Methods*, vol. 11, no. 11, pp. 1099–1103, Nov. 2014, doi: 10.1038/nmeth.3149.

[2] M. E. J. Obien, K. Deligkaris, T. Bullmann, D. J. Bakkum, and U. Frey, "Revealing neuronal function through microelectrode array recordings," *Frontiers Neurosci.*, vol. 8, Jan. 2015, Art. no. 423, doi: 10.3389/fnins.2014.00423.

[3] E. Musk and Neuralink, "An integrated brain-machine interface platform with thousands of channels," *J. Med. Internet Res.*, vol. 21, no. 10, Oct. 2019, Art. no. e16194, doi: 10.2196/16194.

[4] M. Scanziani and M. Häusser, "Electrophysiology in the age of light," *Nature*, vol. 461, no. 7266, pp. 930–939, Oct. 2009.

[5] A. Torricelli, "Neurophotonics: Non-invasive optical techniques for monitoring brain functions," *Funct. Neurol.*, vol. 29, no. 4, pp. 223–230, 2014.

[6] A. Habib, X. Zhu, U. I. Can, M. L. McLanahan, P. Zorlutuna, and A. A. Yanik, "Electro-plasmonic nanoantenna: A nonfluorescent optical probe for ultrasensitive label-free detection of electrophysiological signals," *Sci. Adv.*, vol. 5, no. 10, Oct. 2019, Art. no. eaav9786.

[7] M. Asplund *et al.*, "Toxicity evaluation of PEDOT/biomolecular composites intended for neural communication electrodes," *Biomed. Mater.*, vol. 4, no. 4, Aug. 2009, Art. no. 045009.

[8] I. Posadas, S. Monteagudo, and V. Ceña, "Nanoparticles for brain-specific drug and genetic material delivery, imaging and diagnosis," *Nanomedicine*, vol. 11, no. 7, pp. 833–849, Apr. 2016.

[9] J. Rivnay, H. Wang, L. Fenno, K. Deisseroth, and G. G. Malliaras, "Next-generation probes, particles, and proteins for neural interfacing," *Sci. Adv.*, vol. 3, no. 6, Jun. 2017, Art. no. e1601649.

[10] N. Joye, A. Schmid, and Y. Leblebici, "Electrical modeling of the cell–electrode interface for recording neural activity from high-density microelectrode arrays," *Neurocomputing*, vol. 73, nos. 1–3, pp. 250–259, Dec. 2009.

[11] M. Caglar *et al.*, "All-optical detection of neuronal membrane depolarization in live cells using colloidal quantum dots," *Nano Lett.*, vol. 19, no. 12, pp. 8539–8549, Dec. 2019.

[12] H. Wan *et al.*, "A bright organic NIR-II nanofluorophore for three-dimensional imaging into biological tissues," *Nature Commun.*, vol. 9, no. 1, pp. 1–9, Dec. 2018.

[13] K. Ladutenko, U. Pal, A. Rivera, and O. Peña-Rodríguez, "Mie calculation of electromagnetic near-field for a multilayered sphere," *Comput. Phys. Commun.*, vol. 214, pp. 225–230, 2017.

[14] O. Peña and U. Pal, "Scattering of electromagnetic radiation by a multilayered sphere," *Comput. Phys. Commun.*, vol. 180, no. 11, pp. 2348–2354, 2009.

[15] S. Hsiung Chang, C.-H. Chiang, F.-S. Kao, C.-L. Tien, and C.-G. Wu, "Unraveling the enhanced electrical conductivity of PEDOT: PSS thin films for ITO-free organic photovoltaics," *IEEE Photon. J.*, vol. 6, no. 4, Aug. 2014, Art. no. 8400307.

[16] Y. Du, X. Cui, L. Li, H. Tian, W. X. Yu, and Z. X. Zhou, "Dielectric properties of DMSO-doped-PEDOT: PSS at THz frequencies," *Phys. Status Solidi*, vol. 255, no. 4, 2018, Art. no. 1700547.

[17] M. Oheim, E. Beaurepaire, E. Chaigneau, J. Mertz, and S. Charpak, "Two-photon microscopy in brain tissue: Parameters influencing the imaging depth," *J. Neurosci. Methods*, vol. 111, no. 1, pp. 29–37, 2001.

[18] E. M. Izhikevich, "Simple model of spiking neurons," *IEEE Trans. Neural Netw.*, vol. 14, no. 6, pp. 1569–1572, Nov. 2003.

[19] C. E. Rowland *et al.*, "Electric field modulation of semiconductor quantum Dot photoluminescence: Insights into the design of robust voltage-sensitive cellular imaging probes," *Nano Lett.*, vol. 15, no. 10, pp. 6848–6854, Oct. 2015.

[20] J. D. Marshall and M. J. Schnitzer, "Optical strategies for sensing neuronal voltage using quantum dots and other semiconductor nanocrystals," *Acs Nano*, vol. 7, no. 5, pp. 4601–4609, 2013.

Neuro-SWARM^3: System-on-a-Nanoparticle for Wireless Recording of Brain Activity

Neil Hardy, *Graduate Student Member, IEEE*, Ahsan Habib, *Graduate Student Member, IEEE*, Tanya Ivanov, and Ahmet Ali Yanik, *Member, IEEE*

***Abstract*— A fundamental limitation of the implantable brain-machine interfaces (BMI) is the wiring requirements for power transfer and signal transmission. Existing microelectrode technologies can only record from localized sections of the brain and require implantation of invasive electrodes through cranial surgeries. Here, we introduce a system-on-a-nanoparticle probe, a Neurophotonic Solution-dispersible Wireless Activity Reporter for Massively Multiplexed Measurements (Neuro-SWARM^3), enabling remote detection of *in vivo* bioelectric signals. Neuro-SWARM^3 offers five fundamental advancements simultaneously: (1) it enables use of infrared light within the biologically transparent near infrared (NIR-II, 1000-1700 nm) window for direct read-out through the skull, (2) it circumvents invasive surgical operations since no wiring or power supply is needed for the wireless (electro-plasmonic) excitation and remote detection, (3) due to its diminutive dimensions (<200 nm) that is comparable to viral particles, it can be delivered different regions of the brain without surgical operations, (4) as electro-plasmonic signal conversion removes front-end signal processing requirements, it opens the door to large scale *in vivo* measurements that are not restricted by electrode dimensions, physical wiring, and electronic bandwidth limitations, (5) by being much smaller than the critical dimensions that trigger glial cell response (~12 μm), it offers a long term operation capability. As we show below, NeuroSWARM^3 provides high signal to shot noise ratio (SSNR ~10^3) wireless recording capability from single neurons due to its enhanced scattering cross-section (~10^4 nm^2) and field-sensitivity (up to ~40%).**

***Index Terms*— Neurophotonics, brain–machine interfaces, plasmonics, electrochromic devices, wireless biosensors, biomedical electrodes.**

I. Introduction

UNDERSTANDING how the human brain performs complex functions is one of the greatest scientific, engineering, and medical challenges of the 21st century. It requires a system level approach unraveling how millions of neurons communicate with each other across different anatomical regions of the brain with varying temporal and spatial characteristics and connection strengths. Recording brain activity with high spatiotemporal resolution and in a massively multiplexed manner remains technologically distant. Advancement of fundamentally new detection mechanisms is needed. Electrode arrays, the gold standard for cortical recordings, offer multiplexed electrophysiological recordings with high temporal resolution. However, their use is inherently limited to a few hundred electrodes as direct electronic measurements suffer from complex wiring requirements and inherent bandwidth (spatial multiplexing) limitations due to electron-electron interactions within conductors [1]–[3]. Moreover, electrode arrays can only record from small sections of the brain and require invasive cranial surgical operations [1]. Recent discovery of genetically encoded voltage sensitive fluorescence indicators (GEVI) has created tremendous excitement as light offers unparalleled (wavelength/time/space division) multiplexing and information carrying capabilities [4]. This technique, on the other hand, cannot be implemented in human studies as it requires genetic incorporation of voltage sensitive molecules to neurons. In addition, strong attenuation of visible light in biological tissue renders much of the brain inaccessible to fluorescence-based techniques. Functional near infrared spectroscopy (fNIRS) overcomes visible light limitations and provides non-invasive (non-surgical) volumetric readout of the brain activity as the near infrared (NIR) light can penetrate through the skull into the celebral cortex. fNIRS, on the other hand, can only measure local variations in the cerebral blood volume and oxygenation dynamics, not the electrophysiological signals (action potentials) [5].

In this letter, we introduce a system-on-a-nanoparticle probe, Neuro-SWARM^3, enabling non-invasive detection of *in vivo* electrophysiological activity using near-infrared light. Neuro-SWARM^3 converts bioelectric field oscillations to an optically detectable signal that can be picked up from outside the brain using near-infrared (NIR-II, 1000-1700 nm) light. Much like the passive radio frequency identification (RFID) tags, Neuro-SWARM^3 reports the spiking activity of cells by modulating the incoming NIR light coupling and the re-radiated light spectrum that is sent back to the reader (detector), a method called *backscattering* in radio frequency (RF) engineering. Here, the spectrum of the backscattered NIR light is modulated by the electrochromic loading of the plasmonic (electro-plasmonic) nanoantenna, which shows strong sensitivity to the local electric-field dynamics [6]. Hence, Neuro-SWARM^3 provides a far-field bioelectric signal detection capability in a single nanoparticle device that packs

Manuscript received February 9, 2021; revised May 21, 2021; accepted June 6, 2021. Date of publication June 28, 2021; date of current version July 29, 2021. This work was supported in part by the National Science Foundation, U.S., through the CAREER Award under Grant ECCS-1611290 and Grant ECCS-1847733. *(Neil Hardy and Ahsan Habib contributed equally to this work.) (Corresponding author: Ahmet Ali Yanik.)*

The authors are with the Jack Baskin School of Engineering, University of California at Santa Cruz, Santa Cruz, CA 95064 USA (e-mail: yanik@ucsc.edu).

Color versions of one or more figures in this letter are available at https://doi.org/10.1109/LPT.2021.3092780.

Digital Object Identifier 10.1109/LPT.2021.3092780

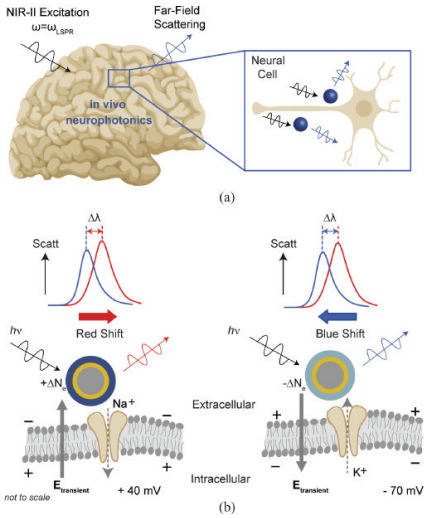

Fig. 1. (a) NeuroSWARM^3 enables remote detection of neural cell activity using NIR-II light far-field scattering. (b) Cell depolarization (spiking) causes a high transient electric field leading to increased light scattering and red shifting of the electro-plasmonic (electrochromic-plasmonic) nanoantenna resonance spectrum. Return to resting potential (repolarization) results in reversal of the scattering spectrum changes.

wireless powering, electrophysiological signal detection and data broadcasting capabilities at nanoscale dimensions.

II. Neuro-SWARM^3 for Brain Activity Imaging

The working principle of Neuro-SWARM^3 is summarized in Fig. 1. In contrast to fNIRS, Neuro-SWARM^3 enables direct measurement of the local electric-field dynamics (neural depolarization events) through NIR light. It uses two fundamental mechanisms for electro-optic translation: (1) drastically enhanced light-matter interactions through localized surface plasmon (LSP) excitation, and (2) enhanced electro-optic sensitivity to local electric-field dynamics through the electrochromic loading of poly(3,4-ethylenedioxythiophene): polystyrene sulfonate (PEDOT:PSS) [6]. PEDOT:PSS outer layer is biocompatible and do not exhibit cytotoxicity as shown in a previous study focused on rodent cortex [7]. Furthermore, Neuro-SWARM^3, a nanoscale probe that is smaller than 200 nm in diameter, can be functionalized with lipid coatings and injected into the circulatory system to be delivered across the blood-brain barrier via receptor mediated transcytosis [8]. Fig. 1a depicts the proposed swarm-and-lock concept schematically. Neuro-SWARM^3 are first distributed within the cortical region of the brain and tethered to specific cell membranes through the surface functionalized proteins (Fig. 1a, inset). Subsequently, far-field scattering signal from the Neuro-SWARM^3 is employed to detect the neural activity, the transient electric field oscillations created by the discharging neuron. During a depolarization event, the membrane potential is controlled by the ionic current, that is sodium (Na^+) and potassium (K^+) movement through the cell membrane (Fig. 1b). Large fluctuations in the membrane potential occur as a result of Na^+ influx into the cell (spike or depolarization phase) and K^+ efflux from the cell (repolarization phase) [9]. Such large charge density (ion concentration) perturbations can give rise to strong transient electric fields ($E_{transient}$). One can estimate the strength of $E_{transient}$ outside the cellular membrane using a charge transfer model. A neural cell can be treated as a 20 μm diameter spherical lipid bilayer with a specific capacitance $C_m = 1$ μF/cm^2 [10]. For a transmembrane potential variation of ~110 mV (Fig. 1b), the total charge that is moved across a cell membrane during a spiking event can be calculated as in $\Delta Q = C_m A_{cell} \Delta V_m$. Here, A_{cell} is the total surface area of the cellular membrane, and ΔV_m is the change in the membrane potential. Such a charging event requires 8.6 million monovalent Na^+ ions to rush into the cell during the spiking phase. One can calculate the instantaneous extracellular electric field strength right outside the cell using this extra charge and the dielectric constant ($\varepsilon_{CSF} = 88.9$) of the cerebrospinal fluid. This model, although simple, accurately captures the extracellular field values, which are typically few tens of mV/nm in strength [11]. Such large extracellular electric-fields can lead to strong modulations in the backscattering signal of Neuro-SWARM^3, enabling far-field detection, as illustrated in Fig. 1b.

III. Field Sensitivity

Neuro-SWARM^3 (SiO_x core radius of 63 nm, 5 nm thick Au shell) is designed to exhibit plasmonic resonance scattering at 1050 nm, corresponding to a wavelength regime enabling deep tissue penetration [12]. A spherically symmetric structure is chosen to minimize the polarization dependence. We used Mie theory for the multilayered core-shell structure calculations [13], [14]. Dielectric constant of the conducting polymer load (PEDOT:PSS) is incorporated using Drude's model [15] with parameters derived from experimental measurements [16]. Electro-optic response of the conducting polymer is incorporated using a similar approach detailed in an earlier work on lithographically fabricated *in vitro* electro-plasmonic nanoantenna [6]. Briefly, a plasma frequency modulation of $\Delta\omega_p = (\omega_p/2N) \times \Delta N$ is assumed for the dielectric load, where ΔN is the surface charge density variation due to a transient extracellular electric field. Such an analytical treatment of the PEDOT:PSS load was validated in an earlier experimental *in vitro* study using visible light and cultured electrogenic cells [6]. In this letter, unlike *in vitro* electro-plasmonic probes, the Neuro-SWARM^3 is designed as a colloidal core-shell electro-plasmonic structure for (i) operability at the NIR frequencies and (ii) non-invasive far-field detection of the *in vivo* electrophysiological signals. We calculated the scattering efficiency for electric field strengths ranging from 0 mV/nm to 12 mV/nm with increments of 4 mV/nm (Fig. 2). Neuro-SWARM^3 demonstrated a scattering efficiency modulation over 20% for an electric field of 12 mV/nm at LSP resonance wavelength

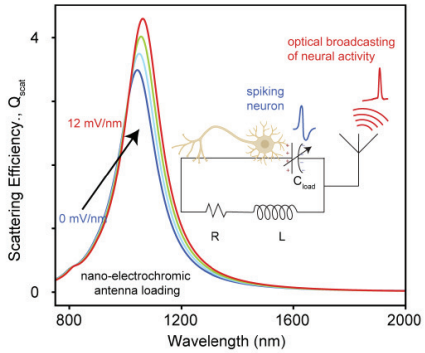

Fig. 2. Optical scattering efficiency, Q_{scat}, spectra for silica-gold nanoshells loaded with PEDOT: PSS. Electric field dependence is shown for 0-12 mV/nm with increments of 4 mV/nm. A core-shell nanoparticle with 63 nm silica core radius, 5 nm thick gold shell, and 15 nm thick PEDOT: PSS coating is considered. Inset shows an equivalent "lumped" optical nanocircuit model of the Neuro-SWARM^3. Local electric-field signal (cell spiking) is translated to the nanoantenna backscattering spectrum through the capacitive (PEDOT:PSS) loading effects.

at ~1050 nm. Electro-optic modulation up to ~40% is also observed at off-resonance wavelengths (~1200 nm), albeit with a lower photon count signal. Electro-optic response of the Neuro-SWARM^3 can be understood following a lumped optical nanocircuit model for the electrochromic polymer (PEDOT:PSS)-nanoantenna system. The electrochromic load, acting as an electric field-controlled nano-capacitor C_{load}, translates the extracellular electric-field dynamics to a scattering signal modulation, as shown in Fig. 2 inset.

We analyzed the scattering signal dependence on PEDOT:PSS layer thickness (Fig. 3). Conventionally, thicker electrochromic films are needed to achieve a strong electro-optic differential signal, which leads to slower temporal response. Neuro-SWARM^3 realizes faster response times and strong signal modulations simultaneously using enhanced light-matter interactions in nanoscale electromagnetic 'hotspots' around the plasmonic core-shell structure (Fig. 3 bottom right inset) [6]. In an earlier work, we experimentally demonstrated that sub-millisecond switching times down to ~200 μs are achievable using a ~20 nm thick PEDOT layer on lithographically fabricated electro-plasmonic nanodisk antenna [6]. In a typical optical system, the differential optical signal (photon count) can be calculated as in

$$\Delta N_{ph} = I_{inc} \left(\Delta Q_{sca} \pi r^2 \right) \left(\lambda / hc \right) \eta T \; t_{\text{int}} \qquad (1)$$

where ΔQ_{sca} is the change in the scattering cross section, I_{inc} is the incident light intensity (10 mW/mm^2), η is the solid angle fraction of the total scattered light collected by a microscope objective (assuming a 20× obj., NA = 0.9) [17]), T is the detection efficiency (quantum yield 0.5), t_{int} is the integration time (1 ms), c is the speed of light, h is Planck's constant, r is the radius of the Neuro-SWARM^3,

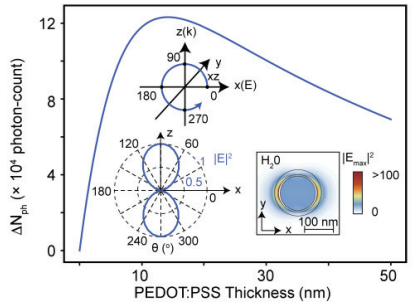

Fig. 3. Differential scattering signal for NeuroSWARM^3 with varying PEDOT:PSS load thickness. The polar plot of the angular scattering by the nanoprobe for linearly polarized incident light (1050 nm) in the x direction is shown in the bottom left (inset). The top inset illustrates how the scattering angle is defined within the xz plane. Electromagnetic "hotspots" due to plasmonic hotspots at 1050 nm are shown in the bottom right (inset). Finite difference time domain (FDTD) calculations were employed to calculate angular scattering and cross-sectional field profile.

and λ is the probing wavelength. As shown in Fig. 3, a single Neuro-SWARM^3 loaded with a thin layer of 5-20 nm PEDOT:PSS can generate a large differential signal (~120 k photons) that can be readily detected. Decreasing scattering signal with increasing PEDOT:PSS thickness beyond ~20 nm is due to the de-tuning of the electro-plasmonic resonance and probing wavelength (1050 nm) with increasing dielectric loading.

IV. High Signal to Noise Ratio Measurements

We demonstrated the functionality of the NeuroSWARM^3 for label-free optical detection of depolarization events using an Izhikevich model for a neuron. Constant voltage pulses (1 mV, 10 ms) were provided as an input at pseudo-random times such that inputs averaged 10 Hz, and model parameters were set such that the neuron exhibits phasic spiking (Fig. 4, black) [18]. Results were generated in 0.1 ms steps and data was compressed by taking the maximum every ten points to preserve relative spike amplitudes for 1 ms integration times. The extracellular field is largely determined by the flow of ions across the cell membrane during spiking. At rest, ionic layer around the membrane surface screens nearly all electric field. However, strong transient electric fields are created during the depolarization and repolarization events as discussed in Section II. As the cell membrane acts as a (dis)charging capacitor, we approximate this field by taking the derivative of membrane voltage with respect to time $I \propto dV/dt$ and adjusting the amplitude of the resulting field to 3 mV/nm, a conservative maximum field estimate according to a previous study [11]. In Fig. 4, we compared the Neuro-SWARM^3 differential signal with that of CdSe quantum dots (QDs), which have recently received significant attention as high photon count alternatives to GEVIs [19]. Differential fluorescence provided by a QD due to an external electric field can be expressed as in $\Delta F/F_0 = -\Delta\tau_r/\tau_r(1 - \Phi_F)$, where $\Phi_F = 0.5$ is the quantum efficiency and $\Delta\tau_r/\tau_r = 0.5\%$